

## CONTACTLESS PNEUMOELECTRIC FLUID VISCOSITY MEASUREMENT DEVICE

A. P. Savenkov, M. M. Mordasov, and V. A. Sychev

UDC 532.137:53.082.36

*We review a variety of contactless techniques for fluid viscosity measurement. We discuss contactless aero-hydrodynamic techniques capable of providing high-accuracy viscosity measurements for non-homogeneous and non-transparent fluids over the range 2–100 Pa·s. We describe a very promising approach in need of additional work—a contactless aero-hydrodynamic technique that involves using a pulsed gas jet to distort the surface of the fluid being measured and determining the viscosity based on the time required to reach a specified deformation level after the gas jet comes on. We have developed a contactless aero-hydrodynamic device with a laser triangulation detector to measure the range to the surface of the liquid; this viscosity measurement device supports full automation, while providing a significant increase in measurement accuracy. We studied four possible options for implementation of the device, and selected the best option to improve the measurement accuracy and reduce the sensitivity of the device to external effects. We describe the design and operating principle for the device, and describe how device design parameters affect systematic and random measurement error. The relative measurement error in fluid viscosity was 2% or less over the entire range from 2 to 100 Pa·s. This contactless aero-hydrodynamic device will be useful for measurement of viscous fluids in a wide variety of industrial fields.*

**Keywords:** *aero-hydrodynamic technique, contactless technique, viscosity, gas, fluid surface, jet, triangulation detector.*

**Introduction.** Viscosity is an important physical property of a fluid, and is used in quality assessment of many products and manufacturing processes in a variety of industrial fields. Measuring the properties of viscous fluids is a complex, lengthy process that involves filling measurement tanks, removing gas bubbles, and cleaning measurement tools, with this last operation frequently requiring toxic and flammable substances. Contactless techniques and devices make inspecting viscous fluids much easier. Contactless techniques for measurement of fluid viscosity include wave techniques, optical techniques, aero-hydrodynamic techniques, and techniques based on capillary waves and levitating drops [1].

The properties of fluids whose surface is covered by surfactant films are traditionally measured using capillary waves [2], which are produced by mechanical vibration of a vessel containing the fluid under study, or by electric fields, acoustic waves, or gas jets [2–4]. The fundamental problem with capillary-wave-based techniques is that fluid density affects the results, and rapid [viscous] damping of capillary waves means that it is difficult to perform viscosity measurements in fluids with viscosities greater than 0.1 Pa·s. Fluid measurement techniques based on the parameters of light scattering from surface capillary waves produced by thermal movement of molecules form a separate group [5, 6]. Due to the short wavelengths of light involved, devices using this technique have an upper measurement limit of 10 mPa·s.

Containerless techniques based on levitating drops have one specialized application—measuring the properties of supercooled metastable melts [7]. The droplet of material for study is lifted up from a support via electrostatic, electromagnetic, aerodynamic, or acoustic levitation [8–12]. These techniques are recommended for use under weightless conditions, but make no sense for ordinary liquids in vessels.

Acoustic and UHF viscosity measurement techniques are based on how wave parameters are affected as waves pass through the layer of fluid being measured [1, 13]. Such techniques are considered contactless if no connection to the process vessel or pipeline is required, and if the wave is transmitted to the fluid being measured through the wall of the vessel or pipeline [14]. The large number of factors affecting the results and the complex interactions between these factors significantly increases the measurement uncertainty for viscosities determined using wave techniques [1]. Optical correlation techniques and techniques based on thermocapillary convection also have similar deficiencies [15, 16].

Reliable viscosity data can be obtained for viscosities ranging from a few tenths to hundreds of Pascal-seconds using contactless methods that involve distorting the surface of the fluid with a laser beam or gas jet [17–19]. Optical methods measure the viscosity of a nanometer-thick surface layer. Due to contamination, this layer may have quite different properties from the bulk fluid being measured. In aero-hydrodynamic techniques, the measured viscosity applies to a fluid layer a few millimeters thick. Aerodynamic techniques have the advantage of easy implementation, and the effects of density and surface tension on the viscosity measurements are smaller.

The most promising aero-hydrodynamic technique involves directing a pulsed gas jet toward the fluid at an oblique angle; this technique shows promise because it makes it much easier to use aerodynamic or optical sensors to determine the extent to which the fluid is distorted by the gas jet [20, 21]. Optical triangulation detectors can also be used to measure the range to the fluid being measured [22]. This enables the components of the measuring device to be precisely adjusted to a specified distance above the surface of the fluid, as required in order to improve the accuracy of the viscosity measurements [23].

The purpose of this paper is to describe the underlying operating principles for a contactless pulsed aero-hydrodynamic viscosity measurement device using a differential laser triangulation detector to measure the distance to the surface of the fluid, evaluate various device design options, and determine the metrological characteristics of the device.

**Aero-hydrodynamic technique and fluid viscosity measurement device.** Figure 1 shows the design of the contactless fluid viscosity measurement device. The following basic components of the measuring device are located above the surface of the fluid: a jet tube JT, which includes a gas-jet nozzle GN and a triangulation detector TD, which in turn consists of a TXL04 laser diode LD (Komoloff, Russia) and BPW34 photodiodes PD1 and PD2 (Vishay Intertechnology Inc., Germany). The operating principle and design for the triangulation detector are described in [23]. The design has been enhanced, with photodiodes being used in place of photoresistors. The TD printed circuit board and GN tube are mounted on a bar that is mechanically connected to the drive D, which moves the bar vertically.

The jet tube receives compressed air from a pneumatic supply line through an RDV5M reduction valve RV (TIZPRIBOR, Russia), a P1PR.5 solenoid valve SV (TIZPRIBOR, Russia), and a laminar-flow orifice LO. The pressure  $p$  upstream of the gas jet nozzle is controlled by reduction valve RV and adjusted based on the readings from M-1/4 manometer MN and the MPX5010DP calibrated pressure transducer PT (Motorola Inc., USA) which is installed immediately upstream of the intake of jet tube JT. The device is controlled by control unit CU, which is based on an ATmega16A microcontroller (Microchip Technology Inc., USA).

In its initial position, the bar carrying jet tube JT and detector TD are relatively far from the surface of the fluid. There are no signals at the TD output. In response to the CU control signal, drive D lowers the bar, and nozzle GN is placed a specified distance  $H$  above the surface of the fluid (the algorithm is described in [23]). In order to reduce the random error in placement of nozzle GN, the bar is moved vertically up and down in the vicinity of the position where the laser beam reflected from the surface of the liquid falls on the boundary between the surfaces of photodiodes PD1 and PD2. Once these sensor elements are in the required position, the LD beam reflected from the surface of the fluid will be incident on the surface of photodiode PD1.

When measuring the viscosity, a signal from control unit CU causes solenoid valve SV to open, and compressed air passes through laminar-flow orifice LO into the JT tube. The zero point for  $t$ , the duration of exposure to the gas stream, corresponds to the point in time at which the pressure at the PT intake reaches a threshold value of 550 Pa. The gas jet from nozzle GN forms an indentation and a wave on the surface of the fluid. The indentation size increases with time, and the wave propagates over the surface of the fluid in the direction of gas flow at a speed that depends on the viscosity  $\eta$  of the fluid. When the wave reaches the point where the beam from laser diode LD hits the fluid surface, this affects the direction of the reflected beam. The TD detector successively produces three states in the discrete output signals  $U_1$  and  $U_2$ :  $U_1 = 1$ ,  $U_2 = 0$  – the reflected beam is primarily incident on the surface of PD1;  $U_1 = 0$ ,  $U_2 = 0$  – the light fluxes incident on PD1 and PD2 are

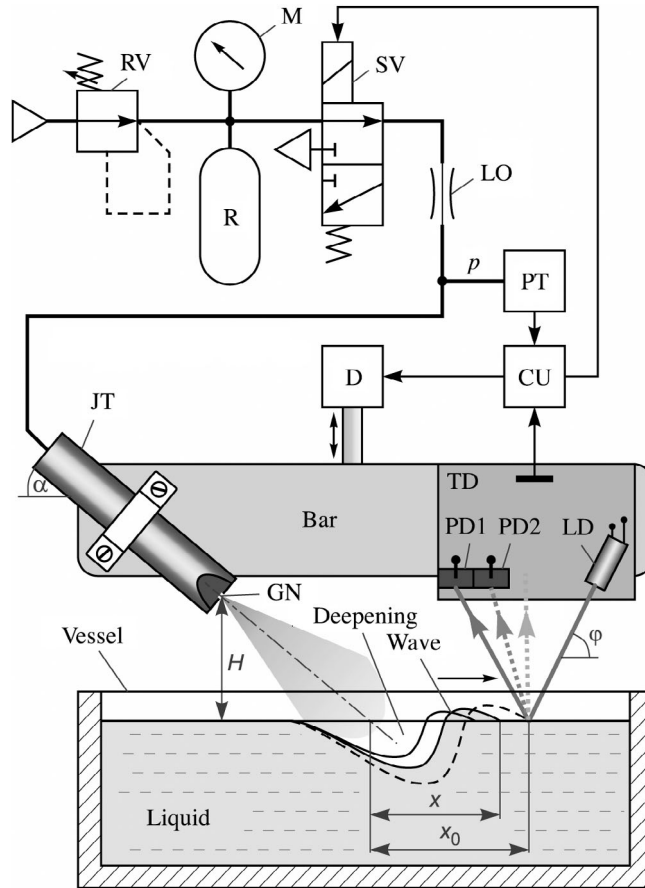


Fig. 1. Diagram of contactless pneumoelectric fluid viscosity measurement device: JT – jet tube; PD1, PD2 – photodiodes; LD – laser diode; GN – gas outlet nozzle; CU – control unit; LO – laminar flow orifice (pneumatic resistance); RV – reduction valve; M – manometer; D – drive; PT – pressure transducer; SV – solenoid valve; R – receiver (50 ml); TD – triangulation detector.

approximately equal;  $U_1 = 0$ ,  $U_2 = 1$  – the reflected beam is primarily incident on the surface of PD2. The CU records the times  $t_1$  and  $t_2$  for the trailing edge of signal  $U_1$  and the leading edge of signal  $U_2$ , respectively. At time  $t_2$ , the CU issues a signal to stop the flow of air to the JT. The fluid viscosity is determined using the arithmetic mean  $t_{12}$  of the quantities  $t_1$  and  $t_2$ . The pressure  $p$  is measured by transducer PT for the entire time  $t_2$  that the gas jet acts on the surface of the fluid. The data on the mean pressure  $p$  is required in order to compensate for the effect of pressure variations on the measured viscosity.

Following a time delay proportional to the time for which the gas jet was active and to the time required for the fluid surface to return to its initial flat state, the viscosity measurement is repeated the specified number of times in order to reduce the effect of random error on the measured result. The viscosity value (equal to the arithmetic mean of the results from the repeated observations) is output to the CU screen.

**Selection of option used for implementation of aero-hydrodynamic viscosity measurement device.** The differential triangulation detector (TD) enables the specified distance  $H_s^0$  above the surface of the fluid to be measured to within 0.1 mm (Fig. 2, zero position) [22, 23]. However, the viscosity should not be measured in the zero position, since even minor changes in the shape of the fluid surface will trip the TD. In the zero position, the fluid surface deformation time tends to zero, the effect of fluid density on the measured results becomes comparable to that of viscosity, and the random component of the error increases (Fig. 3). In order to improve the noise immunity of the device, the TD must be moved either above or below zero position prior to initiating the gas flow. This observation implies that there are four options for implementing the device depending on the direction of the gas jet and the laser beam (see Fig. 2).

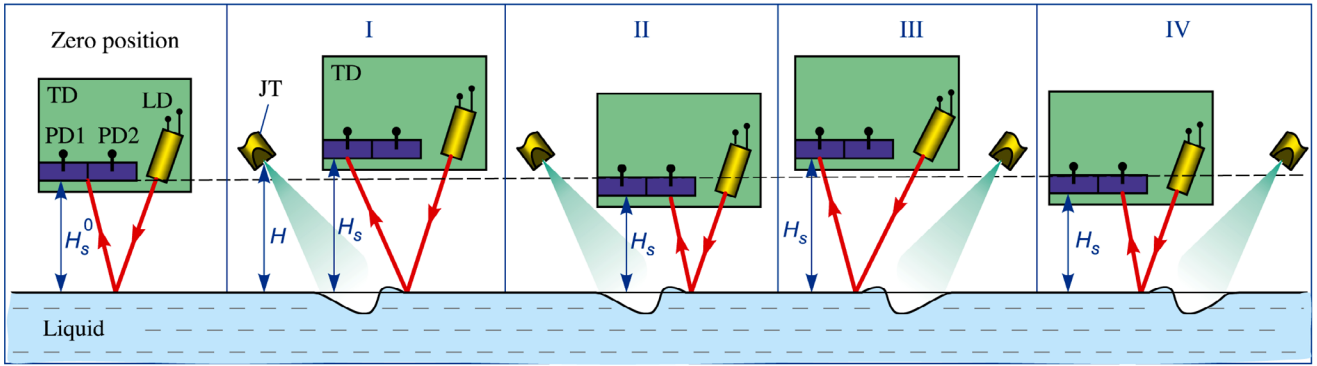


Fig. 2. Options I–IV for an aerohydrodynamic viscosity measurement device with the gas jet and laser beam pointing in opposite directions (I, II) or the same direction (III, IV); symbols identical to those in Fig. 1.

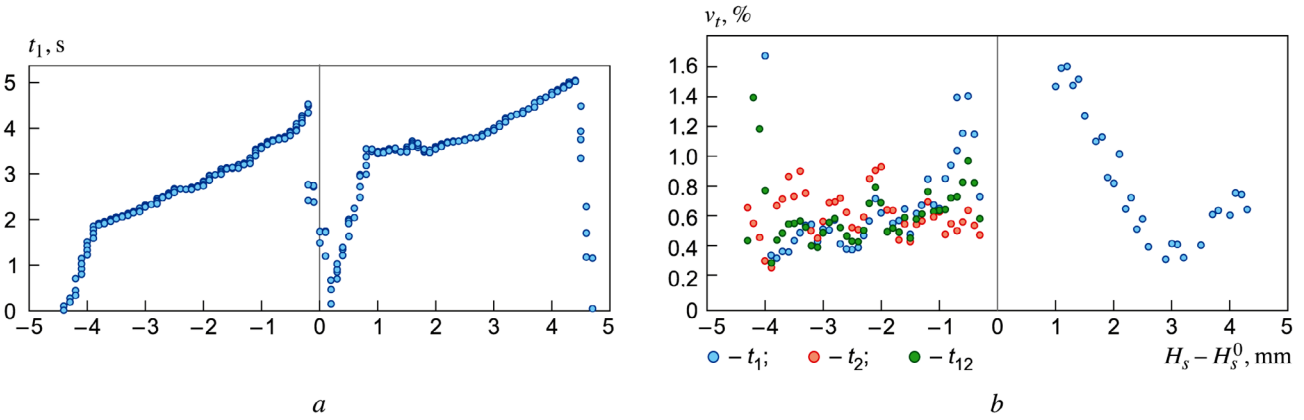


Fig. 3. Fluid surface deformation time  $t_1$  (a) and coefficients of variation  $v_t$  of time intervals (b) as a function of the position of the triangulation detector.

*Option I.* Laser beam and gas jet point in opposite directions. TD position  $H_s > H_s^0$ . Advantages: two time intervals  $t_1$  and  $t_2$  can be used; the distance  $H$  has a weak effect on the measured results; and the linear shift is sensitive to the depth of the indentation. Disadvantages: none.

*Option II.* Laser beam and gas jet point in opposite directions. TD position  $H_s < H_s^0$ . Advantages: none. Disadvantages: only one time interval  $t_1$  can be used; the distance  $H$  has a significant effect on the measured results; and the linear shift is insensitive to the depth of the indentation.

*Option III.* Laser beam and gas jet point in the same direction. TD position  $H_s > H_s^0$ . Advantages: the distance  $H$  has a weak effect on the measured results; and the linear shift is sensitive to the depth of the indentation. Disadvantages: only one time interval  $t_1$  can be used.

*Option IV.* Laser beam and gas jet point in the same direction. TD position  $H_s < H_s^0$ . Advantages: two time intervals  $t_1$  and  $t_2$  can be used. Disadvantages: the distance  $H$  has a significant effect on the measured results; and the linear shift is insensitive to the depth of the indentation.

Options I, III, and IV were selected for experimental study; Option II turned out to be unpromising, and was not studied. The design parameters of the device were as follows (see Fig. 1): angle between jet and fluid surface  $\alpha = 20^\circ$ ; distance from GN nozzle to fluid surface  $H = 10.3$  mm; diameter of GN nozzle  $d = 0.89$  mm; orifice coefficient of nozzle  $\mu = 0.68$ ; pressure upstream of GN nozzle  $p = 5.45$  kPa.

TD parameters:  $\varphi = 60^\circ$ ;  $H_s^0 = 8$  mm. The design permits horizontal movement of the TD in order to vary the distance  $x_0$  that the wave travels over the surface of the fluid before reaching the point where the laser beam hits the surface. Values of  $x_0 = 20.5$ ,  $20.5$ , and  $15.5$  mm were selected for Options I, III, and IV, respectively; these values maximize the

distance  $x$  that the wave propagates over the surface of the fluid, while permitting stability of device operation. The distance that the wave propagates must be increased in order to reduce the effect of fluid density and surface tension on the measured viscosity, since viscosity has the largest impact on wave propagation.

Figure 3a shows the deformation time  $t_1$  for the fluid surface as a function of TD position for the case where the gas jet and laser beam are pointing in the same direction (Options III and IV). The distances  $H_s$  and  $H$  (see Fig. 1) were simultaneously varied during the experiments. The distance  $H$  was only equal to the specified value of 10.3 mm at two points where  $H_s - H_s^0 = \pm 2.5$  mm. The TD was moved horizontally whenever the distances  $H_s$  and  $H$  changed, so as to keep the values  $x_0 = 20.5$  and 15.5 mm constant in Options III and IV, respectively. ED-20 epoxy resin (with viscosity  $30 \pm 2$  Pa·s at temperature  $24.2 \pm 0.3^\circ\text{C}$ ) was selected as an experimental fluid.

Figure 3a suggests that the TD responds much more rapidly when the reflected laser-diode beam is incident on the boundary between photodiode surfaces (see Fig. 2), which corresponds to the following conditions:

$H_s - H_s^0 < -4$  mm, beam incident on the right-hand edge of the surface of photodiode PD2 (Option IV);

$H_s - H_s^0 \approx 0$ , beam incident on the boundary between the surfaces of photodiodes PD1 and PD2 (zero position);

$H_s - H_s^0 > 4.5$  mm, beam incident on the left-hand edge of the surface of photodiode PD1 (Option III);

Figure 3b shows the coefficient of variation  $v_t$  (relative standard deviation) for the time intervals  $t_1$  and  $t_2$  and the arithmetic mean  $t_{12}$  of these time intervals as a function of TD position. The curves were constructed using the same experimental data used for Fig. 3a. The data were smoothed using a moving average. The coefficient of variation is the ratio of the root-mean-square deviation to the arithmetic mean, expressed in percent, and in this case, it describes the random component of the error in the viscosity measurements. The coefficient of variation is larger when the laser beam is reflected onto the boundary between the TD photodiode surfaces. Functions similar to those shown in Fig. 3 were also typical of other device implementation options, particularly Option I. The nature of changes in values  $t_1$ ,  $t_2$ ,  $t_{12}$ , and  $v_t$  was not affected by the angle  $\alpha$  or distance  $H$  (see Fig. 1) since it is primarily determined by the TD parameters. A study of various implementation options for the device indicated that the best value for  $H_s$  met the condition  $2.3 \text{ mm} < |H_s - H_s^0| < 2.5 \text{ mm}$ , where the impact of both the random component of the error and the distance  $H$  from the GN nozzle to the fluid surface was the smallest.

Options I and IV enable recording of the two time intervals  $t_1$  and  $t_2$  for deformation of the fluid surface by the gas jet, and the viscosity is determined from the arithmetic mean  $t_{12}$ . Figure 3b implies that using  $t_2$  is better, since the coefficient of variation for this time interval is slightly larger than the coefficient of variation for the time interval  $t_1$ . Using the arithmetic mean  $t_{12}$  would reduce any effect that external illumination and the index of refraction of the fluid might have on the measured results. These factors affect the width of the TD dead zone where the laser fluxes incident on the photodiodes are equal. At lower indices of refraction and higher external light fluxes, the dead-zone width increases with decreasing  $t_1$  and increasing  $t_2$ . The arithmetic mean  $t_{12}$  is much less affected by dead-zone width. Using the two time intervals  $t_1$  and  $t_2$  also reduces the effect of the distance  $H$  on the measured results, since  $t_1(H)$  and  $t_2(H)$  partially compensate for one another in the vicinity of the specified value for  $H$ .

Option I is preferable to Option IV (see Figs. 1 and 2), since it reduces the effect of the distance  $H$  and the density and surface tension of the fluid on the measured viscosity. Simultaneously varying the distances  $H$  and  $H_s$  by 0.1 mm changes the output signal from the device by 0.5%, 0.9%, and 2.7% under Options I, III, and IV, respectively. The distances  $H$  and  $H_s$  have a large effect in Option IV because the relative change in  $H_s$  corresponding to an identical absolute change in the distance (0.1 mm) turns out to be much larger in Option IV than for the other options.

As mentioned above, the effect of fluid density and surface tension on the measured results is due to the fact that these effects are linear functions of the depth of the indentation, which is smallest for Option IV (15.5 mm compared with 20.5 mm for Options I and III). The smaller linear displacement for Option IV is due to the fact that more distortion of the fluid surface is required to trip the TD and the fact that the distance  $H_s$  is smaller. The wave decreases in height as it propagates along the surface of the fluid, meaning that for large values of  $x$ , the laser beam deviation will be insufficient to trigger the TD when  $H_s < H_s^0$  (see Figs. 1 and 2).

This all suggests that Option I is the best option.

**Experimental viscosity measurement error for contactless aero-hydrodynamic device.** The viscosity response functions and measurement-error curves were experimentally determined for Option I. The experiments were performed

TABLE 1. Experimental Viscosity Measurement Error Results Using Contactless Aero-Hydrodynamic Device

Fluid	$\eta_0$ , Pa·s	$t_{12}$ , s	$\eta = -0.294 + 6.950t_{12}$			$\eta = -0.14 + 6.76t_{12}$		
			$\eta$ , Pa·s	$\Delta\eta$ , Pa·s	$\delta_\eta$ , %	$\eta$ , Pa·s	$\Delta\eta$ , Pa·s	$\delta_\eta$ , %
Transmission oil, TSp-15K	0.421 ± 0.003	0.106	<b>0.443</b>	<b>0.022</b>	<b>5.2</b>	0.577	0.156	37.0
Compressor oil, KS-19	0.607 ± 0.005	0.125	<b>0.575</b>	<b>-0.032</b>	<b>5.3</b>	0.705	0.098	16.1
Transmission oil, TAp-15V	0.880 ± 0.005	0.166	<b>0.860</b>	<b>-0.020</b>	<b>2.3</b>	0.982	0.102	11.6
Glycerin	1.055 ± 0.015	0.200	<b>1.096</b>	<b>0.041</b>	<b>3.9</b>	1.212	0.157	14.9
Transmission oil, TEhp-15	2.72 ± 0.02	0.422	2.64	-0.08	3.0	<b>2.71</b>	<b>-0.01</b>	<b>0.3</b>
Transmission oil, motor-vehicle and tractor* (Nigrol)	3.84 ± 0.06	0.578	3.72	-0.12	3.0	<b>3.77</b>	<b>-0.07</b>	<b>1.9</b>
Standard sample, Brookfield 12500	12.20 ± 0.12	1.860	12.6	0.4	3.5	<b>12.4</b>	<b>0.2</b>	<b>1.9</b>
Epoxy resin, EhD-20	26.1 ± 0.3	3.850	26.5	0.4	1.4	<b>25.9</b>	<b>-0.2</b>	<b>0.8</b>
Standard sample, Brookfield 100000	101.8 ± 1.0	15.000	104.0	2.2	2.2	<b>101.3</b>	<b>-0.5</b>	<b>0.5</b>

\* Per GOST 542-50, Transmission Oil, Motor-Vehicle and Tractor. Specifications.

using Brookfield standard viscosity samples, as well as fluids for which the true viscosity values  $\eta_0$  were obtained using a Brookfield viscosimeter calibrated against standard samples (Table 1) [24]. All observations were performed at fluid temperatures of  $25.0 \pm 0.1^\circ\text{C}$ . The duration  $t_{12}$  for which the jet acted on the surface of the fluid was determined via repeated measurement. The fluid densities ranged from  $900 \text{ kg/m}^3$  to  $1300 \text{ kg/m}^3$ . The viscosity  $\eta$  as a function of the time  $t_{12}$  was approximated by two linear functions  $\eta = b_0 + b_1 t_{12}$ , where  $b_0 = -0.294 \text{ Pa}\cdot\text{s}$ ,  $b_1 = 6.95 \text{ Pa}$  for non-viscous fluids ( $\eta \leq 2 \text{ Pa}\cdot\text{s}$ ) and  $b_0 = -0.14 \text{ Pa}\cdot\text{s}$ ,  $b_1 = 6.76 \text{ Pa}$  for viscous fluids ( $\eta > 2 \text{ Pa}\cdot\text{s}$ ). Table 1 lists the experimentally determined viscosity measurement errors for the contactless aero-hydrodynamic device; the boldfaced numbers indicate values obtained by applying the aforementioned calibration curves over the ranges indicated; the italicized numbers indicate values obtained using the approximation to the function  $\eta(t_{12})$  for viscous fluids where the viscosity is  $2 \text{ Pa}\cdot\text{s}$  or less and the error is exceptionally large. Table 1 indicates that when the calibration curve for non-viscous fluids has maximum relative error  $\delta_\eta$  was 6% and 4% in the 0.4–1.0 Pa·s and 1–100 Pa·s ranges, respectively. The calibration function for viscous fluids has relative error  $\delta_\eta < 2\%$  over the range from  $2 \text{ Pa}\cdot\text{s}$  to  $100 \text{ Pa}\cdot\text{s}$ .

**Conclusion.** We were able to experimentally validate the specific option selected for implementation of the aero-hydrodynamic viscosity measurement device and estimate the measurement error. This device provides a relative error of no more than 2% in fluid viscosity over the range from 2 to  $100 \text{ Pa}\cdot\text{s}$  for fluids with densities ranging from  $900$  to  $1300 \text{ kg/m}^3$ . The measurement error is primarily multiplicative in nature. The calibration function is linear and approximately proportional. This contactless aero-hydrodynamic device is useful for testing of viscous fluids, e.g., resins during the hardening process.

We expect to continue this research with development of a mathematical model for the interaction between the gas jet and the fluid surface, and optimization of the device design and operating modes for measurement of non-viscous fluids, with an eye to determining the smallest measurable viscosity and improving the measurement accuracy.

## REFERENCES

1. M. M. Mordasov and A. P. Savenkov, "Contactless techniques for fluid viscosity measurement (review)," *Zavod. Lab. Diagn. Mater.*, **79**, 27–35 (2013).
2. C. H. Sohl, K. Miyano, J. B. Ketterson, *Rev. Sci. Instrum.*, **49**, No. 10, 1464–1469 (1978), <https://doi.org/10.1063/1.1135288>.
3. F. Behroozi, J. Smith, and W. Even, "Stokes' dream: Measurement of fluid viscosity from the attenuation of capillary waves," *Am. J. Phys.*, **78**, No. 11, 1165–1169 (2010), <https://doi.org/10.1119/1.3467887>.
4. B. M. Pierce and D. B. Chang, US Patent 5005401, subm. April 9, 1991.

5. Y. Nishimura, A. Hasegawa, and Y. Nagasaka, "High-precision instrument for measuring the surface tension, viscosity and surface viscoelasticity of liquids using ripplon surface laser-light scattering with tunable wavelength selection," *Rev. Sci. Instrum.*, **85**, No. 4, 044904 (2014), <https://doi.org/10.1063/1.4871992>.
6. T. M. Koller, T. Klein, C. Giraudet, et al., "Liquid viscosity and surface tension of n-dodecane, n-octacosane, their mixtures, and a wax between 323 and 573 K by surface light scattering," *J.Chem. Eng. Data*, **62**, No. 10, pp. 3319–3333 (2017), <https://doi.org/10.1021/acs.jced.7b00363>.
7. D. M. Herlach, R. F. Cochrane, I. Egry, et al., "Containerless processing in the study of metallic melts and their solidification," *Int. Mater. Rev.*, **38**, No. 6, 273–347 (1993), <https://doi.org/10.1179/095066093790326267>.
8. L. H. Li, L. Hu, S. J. Yang, et al., "Thermodynamic properties and solidification kinetics of intermetallic Ni<sub>7</sub>Zr<sub>2</sub> alloy investigated by electrostatic levitation technique and theoretical calculations," *J. Appl. Phys.*, **119**, 035902 (2016), <https://doi.org/10.1063/1.4940243>.
9. J. Brillo, G. Lohöfer, F. Schmidt-Hohagen, et al., "Thermophysical property measurements of liquid metals by electromagnetic levitation," *Int. J. Mater. Prod. Technol.*, **26**, No. 3/4, 247–273 (2006), <https://doi.org/10.1504/IJMPT.2006.009469>.
10. D. Langstaff, M. Gunn, G. N. Greaves, et al., "Aerodynamic levitator furnace for measuring thermophysical properties of refractory liquids," *Rev.Sci. Instrum.*, **84**, 124901 (2013), <https://doi.org/10.1063/1.4832115>.
11. J. Kremer, A. Kilzer, and M. Petermann, "Simultaneous measurement of surface tension and viscosity using freely decaying oscillations of acoustically levitated droplets," *Rev.Sci. Instrum.*, **89**, 015109 (2018), <https://doi.org/10.1063/1.4998796>.
12. V. Ansari Hosseinzadeh and R. G. Holt, "Finite amplitude effects on drop levitation for material properties measurement," *J. Appl. Phys.*, **121**, 174502 (2017), <https://doi.org/10.1063/1.4982908>.
13. F.-J. Kuo, C.-T. Sheng, and C.-H. Ting, "Evaluation of ultrasonic propagation to measure sugar content and viscosity of reconstituted orange juice," *J. Food Eng.*, **86**, No. 1, 84–90 (2008), <https://doi.org/10.1016/j.jfoodeng.2007.09.016>.
14. M. M. Mordasov, A. P. Savenkov, and K. E. Chechetov, "Use of the term 'contactless measurement technique'," *Datch. Sistemy*, No. 4, 47–52 (2017).
15. D. D. Postnov, F. Moller, and O. Sosnovtseva, "Dairy products viscosity estimated by laser speckle correlation," *PLoS ONE*, **13**, No. 9, e0203141 (2018), <https://doi.org/10.1371/journal.pone.0203141>.
16. B. A. Bezuglyi, O. A. Tarasov, and S. I. Chemodanov, Patent No. 2305271 RF, *Izobret. Polezn. Modeli*, No. 24 (2007).
17. Y. Yoshitake, S. Mitani, K. Sakai, and K. Takagi, "Measurement of high viscosity with laser induced surface deformation technique," *J. Appl. Phys.*, **97**, 024901 (2005), <https://doi.org/10.1063/1.1839640>.
18. S. Nowinski, GB Patent 2192987, subm. Jan. 27, 1988.
19. P. G. Backes, US Patent 5024080, subm. June 18, 1991.
20. M. M. Mordasov and A. P. Savenkov, "Pneumatic contactless measurement of fluid viscosity," *Zavod. Lab. Diagn. Mater.*, **75**, No. 2, 33–37 (2009).
21. D. M. Mordasov, M. M. Mordasov, and A. P. Savenkov, *Aero-Hydrodynamic Effects in Contactless Jet Techniques for Nondestructive Fluid Viscosity Measurement*, Fizmatlit, Moscow (2012).
22. M. M. Mordasov, A. P. Savenkov, M. E. Safonova, and V. A. Sychev, "Non-contact triangulation measurement of distances to mirror surfaces," *Avtometriya*, **54**, No. 1, 80–88 (2018), <https://doi.org/10.15372/AUT20180111>.
23. M. M. Mordasov, A. P. Savenkov, V. A. Sychev, and G. V. Mozgova, "Laser triangulation rangefinder for specular surfaces," *Datch. Sistemy*, No. 3, 49–53 (2018).
24. S. V. Mischenko, M. M. Mordasov, A. P. Savenkov, and V. A. Sychev, "Analysis of the influence of sizes of a vessel with a liquid on the readings of Brookfield viscometer," *Izmer. Tekhn.*, No. 4, 33–38 (2020), <https://doi.org/10.32446/0368-1025it.2020-4-33-38>.